Materials Science Forum
ISSN: 1662-9752, Vol. 881, pp 464-470
doi:10.4028/www.scientific.net/MSF.881.464

Submitted: 2016-08-22
Accepted: 2016-08-22
Online: 2016-11-30

The Influence of a Nickel Precursor on the Synthesis of Nanosized NiO Material Using the Hydrothermal Method: Characterization and Electrocatalytic Oxidation of Methanol

Marília Evelyn R. Oliveira[1,a], Francisco Xavier Nobre[2,b], José Ribeiro dos Santos Júnior[1,c] and José Milton Elias de Matos[2,d]

[1]Federal University of Piaui – UFPI /CCN –- Laboratory of Bioelectrochemistry - Campus University Minister Petrônio Portela, Ininga, Teresina – PI, 64049-550, Brazil, phone (550XX86) 3221 5710.

[2]Federal University of Piaui – UFPI/CCN – Department of Chemistry - Interdisciplinary Laboratory for Advanced Materials – LIMAv – Campus University Minister Petrônio Portela, Ininga, Teresina – PI, 64049-550, Brazil, phone (550XX86) 3221 5710.

[a]marilia_evelyn@hotmail.com, [b]xavier.nobre.ufpi@gmail.com, [c]jribeiro@ufpi.edu.br, [d]jmematos@ufpi.edu.br

Keywords: NiO oxides; hydrothermal synthesis; oxidation of methanol

Abstract. Nickel oxide (NiO) was prepared by the hydrothermal method using hydrogen peroxide to form a nickel peroxide complex, and irregular spherical and rod-shaped NiO nanoparticles were obtained. The factors that influence the physical properties of NiO nanoparticles were studied using scanning electron microscopy (SEM), isothermal gas adsorption/desorption by Brunauer, Emmett and Teller (BET), and X-ray diffraction (XRD) techniques. This study found that the precursor salt chosen (nickel acetate or nickel nitrate) significantly affected the shape, particle size, and surface area of the synthesized nanosized NiO powders. The ratio of hydrogen peroxide (H_2O_2) to nickel nitrate or acetate and the heating rate of calcinations were also important in determining the physical properties of the nanosized NiO. The unmodified PAni electrode shows no activity for the methanol oxidation reaction in 0.1 M NaOH. However, the nickel-modified PAni electrode is a good catalyst for this reaction and high current densities can be reached. The height of the oxidation peak of methanol increases by increasing the alcohol concentration. The results indicate that the reaction of the electro-oxidation of methanol is an activation-controlled proceeding by a direct chemical reaction with NiO(OH) for thin nickel oxides and by charge transfer with the electrode for thick oxides.

Introduction

Over the last few years, nanocrystalline materials have been intensively studied due to their exotic physical and chemical properties, which differ from those seen in bulk materials [1, 2]. These unique properties suggest they are of extreme importance and have many potential applications. Nickel oxide (NiO) is a semiconductor and an antiferromagnetic material. NiO nanocrystals with various shapes including nanosheets [3], nanoparticles [4], nanofibres [5], nanotubules [6], nanowires [7], and nanorings [8] have recently been successfully synthesized by different methods. For example, Hyeon *et al.* synthesized NiO and Ni nanoparticles by thermal decomposition of Ni-alkylamine complexes in trioctylphosphine (TOP) [9]. An *et al* obtained a nanocrystalline NiO at a low temperature in a molten solution of mixed KOH/NaOH [10]. A simple method of low cost, low temperature, large-scale, and controlled growth of oxide nanostructures at atmospheric pressure is highly desirable. The authors of this article believe that the hydrothermal method is a highly effective way of synthesizing nano oxides. In this study, NiO nanoparticles are obtained by the hydrothermal method, in the presence of hydrogen peroxide and water as a solvent, using a regular laboratory oven that was maintained at a constant temperature (130 ^{o}C) for 48h and calcinations at 300 ^{o}C/2h. We also report the deposition of NiO and PAni and its activities of methanol oxidation. It also investigates how the experimental parameters influence the physical properties of particles, using BET, FE-SEM, and XRD characterization techniques. The catalytic activity was investigated by cyclic voltammetry.

Experimental

The hydrothermal method was used to prepare the nickel hydroxide. The analytical grade reagents used were: nickel acetate, $Ni(C_2H_3O_2)_2.4H_2O$ (Dinâmica, 99%), and nickel nitrate, $Ni(NO_3)_2.6H_2O$ (Dinâmica, 99%). Nickel salts were dissolved in deionized water, and H_2O_2 (30 wt% solution) was added at a ratio of 15/1% mol H_2O_2/Ni. This solution was poured into a bottle with an autoclavable screw cap. The bottle was then placed in a regular laboratory oven and subjected to a constant temperature (130 $^{\circ}$C) for 48h. Subsequently, the green solution was dried at 100 ^{o}C, and the resultant $Ni(OH)_2$ was converted to NiO by calcination at 300 ^{o}C for 2h, obtaining a dark gray powder.

The NiO were characterized by X-ray diffractometry (Rigaku D-Max 2500 diffractometer with CuKα radiation, in a scanning routine of 1^{o} min^{-1}, to define the peak position and width) in a 2θ range from 10° to 75°. Their size and morphology were inspected with field scanning electron microscopy (FESEM, JEOL 3010). The particle size distribution was estimated based on the measurements of TEM images of at least 200 particles. The TEM samples were prepared by wetting carbon-coated copper grids with a drop of the colloidal suspensions for 20s, followed by air-drying.

PANI was chemically synthesized by chemical polymerization according to a systematic approach [11]. The films were obtained by the Layer-by-Layer (LbL) technique, prepared from an aqueous dispersion of HEC (Hydroxyethyl Cellulose) and the mixture of PANI (emeraldine base) soluble in water and NMP and NiO (NiO-Ac (from nickel acetate) and NiO-Nit (from nickel nitrate), using 2.0 g L^{-1} of each reagent separately and sonicated for 5 min. The LbL films of HEC-PANI, HEC-NiO-Ac/PANI, and HEC-NiO-NIT/PANI were prepared on glass substrates coated with a thin layer of tin oxide doped with indium (ITO) and previously cleaned and hydrophilized.

The composite films were assembled by immersing the substrate alternately into the ITO dispersion of HEC and then into the dispersion of NiO/PANI, which was repeated four more times. After each layer deposition, the substrate was washed for 30 seconds with ultrapure water (Milli-Q), dried with N_2 gas flow. This procedure resulted in the formation of ITO/HEC-(NiO/PANI) films of five bilayers. The films were subsequently applied in the electro-oxidation of methanol in acidic and basic solutions.

Electrochemical experiments were performed at room temperature using a potentiostat/ galvanostat (Autolab, PGSTAT-302) in an electrochemical cell with three electrodes, and the electrode Ag/AgCl (KCl 3.0 mol L^{-1}) as a reference and a platinum blade as an auxiliary electrode. All electrochemical measurements were performed at 100 mV in acidic H_2SO_4 0.05 mol L^{-1} and in alkaline NaOH 0.1 mol L^{-1}.

Results and Discussion

Characterization of NiO

The products that were synthesized using nickel acetate or nitrate ($Ni(OH)_2$) were grey-black in color. In order to obtain NiO nanocrystals, the As-prepared $Ni(OH)_2$ nanoplates, obtained through the hydrothermal method, were calcined. Figure 1 illustrates the XRD patterns of the As-prepared samples after calcination at 300 ^{o}C. The diffractograms that were obtained demonstrate that all the samples can be perfectly indexed to the cubic structure (JCPDS card No. 22-1189) of crystalline NiO and there is no impurity in the powder, which proves that only NiO exists. The powder obtained from both precursors has the same structure, but the crystallographic profile of NiO suggests that the crystallite size is smaller than that from the nitrate salt.

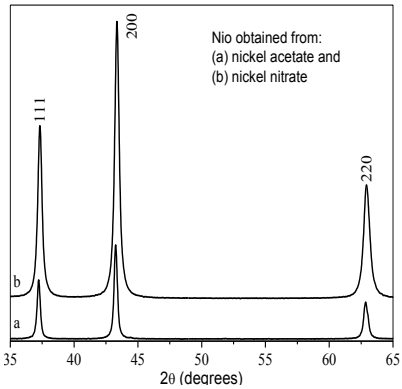

Fig. 1. XRD patterns of NiO obtained after calcinations at 300 °C for 2 h.

Characterization of the microstructure of these nanocrystals is carried out by employing Rietveld's analysis. In the present study, the most suitable pseudo-Voigt analytical function [12] is adopted for fitting the experimental profiles. The XRD patterns have been analyzed using Rietveld analysis providing the volume averaged crystallite size, microstrain, and weight fraction of the detected phases.

Figure 2 (a–c) shows the structural refinement performed on the NiO nanocrystals. To verify and confirm if the structure of NiO nanocrystals is cubic, a structural refinement was performed by the Rietveld method. The results obtained by Rietveld refinement method show a good agreement between the observed XRD patterns and the theoretical results for the cubic structure. Moreover, the difference between the profiles of XRD experimental patterns observed and the theoretical calculated data display small differences near zero in a scale of intensity, as illustrated in Figure 2(a–c) by a line ($Y_{observed} - Y_{calculated}$). In this paper, we have initially applied the Rietveld method or full pattern analysis for structural refinement of NiO nanocrystals.

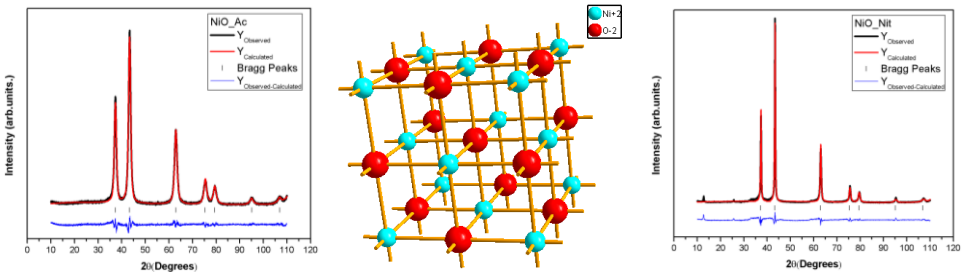

Fig. 2. Rietveld refinement plot of NiO obtained from nickel acetate (a) and nickel nitrate (c) after calcinations at 300 °C for 2 h, and (b) Schematic representation of unit cell illustrating the NiO clusters.

The Rietveld method is a least squares refinement procedure where the experimental step-scanned values are adapted to calculated ones. The profiles are considered to be known, and a model for a crystal structure available [13]. The profiles of the XRD experimental patterns observed for the NiO nanocrystals were refined with a theoretical line profile known as Crystallographic Information File (CIF) [14] related to the respective No. 9866 ICSD (PDF 71-1179) [15]. In the structural refinement performed in Maud program, the Rietveld texture and stress analysis were employed [16]. The quality of a structural refinement is generally checked by *R*-values (R_{wnb}, R_b, R_{exp}, R_{wp}, and σ). Those numbers are easy to communicate being consistent with a cubic structure. However, a difference in plot between observed and calculated patterns is the best way to judge the success of a Rietveld refinement. For all the Rietveld analyses, the R-weighted pattern (R_{wp}), this is a useful indicator of the goodness of the fit. It is close to 10% (6.97% and 14.01% to NiO – acetate and NiO – nitrate, respectively), indicating a rather high reliability of the results. The analysis of the positions and relative intensities of the diffracted lines confirms the presence of the single phase cubic structure of NiO with a space group *Fm3m* and cell parameters a = 4.185(7) Å and 4.177(2) Å and cell volume of V = 73.335 Å^3 (d = 6.768 g cm^{-3}) and 72.889 Å^3 (d = 6.810 g cm^{-3}) to NiO – acetate and NiO – nitrate, respectively.

To NiO obtained from the nickel acetate, the Rietveld method corroborates with XRD results, indicating that a pure nickel oxide was obtained (Fig. 2a). To NiO obtained from the nickel nitrate, the Rietveld method presents a different result, indicating that moisture of nickel oxide containing a little of nickel nitrate as a contaminant was obtained.

The TEM images in Figures 3 show the morphologies of the above-mentioned NiO samples. The 300 ^{o}C-calcined NiO obtained from the nickel acetate (Fig. 3 a and b) has dispersed irregular particles. There is a large quantity of crystals with sizes in the range of 10–90 nm (Fig. 3c). These irregular shapes are probably formed by the escape water that is generated during dehydroxylation of the Ni(OH)$_2$ precursor.

Figure 3 (d and e) illustrates the morphologies of the NiO obtained from the nickel nitrate. The samples are also dispersed in irregular particles. A large quantity of crystals, with sizes in the range of 10–90 nm, was also found (Fig. 3f). Unlike the NiO obtained from the nickel acetate, crystals with nanowire morphologies up to 280 nm long were obtained.

In general, the NiO crystals (shown in detail in Figures 3 a, b, d and e) have no well-determined shape, as one can see in the distribution presented in Figure 3 (c and f). Notably, the average diameter of these rods is around 15 nm (NiO obtained from the nickel acetate) and 25 nm (NiO obtained from the nickel nitrate), which is below the stability size for the cubic phase, as reported in the scientific literature.

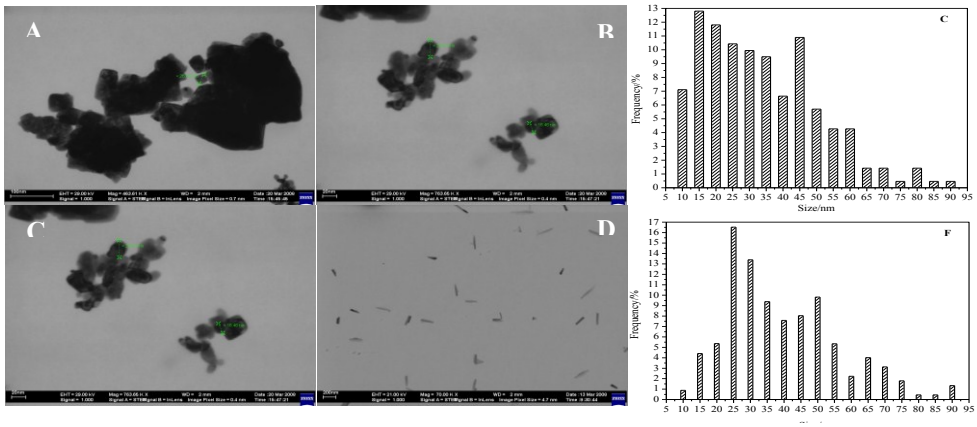

Fig. 3. TEM images of NiO samples obtained from nickel acetate (A and B) and from from nickel nitrate (C and D), after calcination at 300 ^{o}C and, size distribution diagram of the product (C) nickel acetate and (D) nickel nitrate.

The Ni(OH)$_2$ nanosheets, as a precursor, were thermally treated at 300 ^{o}C for 2h in order to convert Ni(OH)$_2$ to NiO. The XRD patterns (and Rietveld method) of the samples shown in Figures 1 and 2, can be indexed to a single phase of cubic NiO. No peaks from the precursor Ni(OH)$_2$ were observed in the XRD pattern, which indicates the complete transformation of Ni(OH)$_2$ to NiO with a little of parent salt (less than 3%) to NiO obtained from the nickel nitrate. In the TEM micrographs of the two samples presented in Fig. 3, the crystals were more irregular than those found in other studies [10]. We believe that the lack of a defined shape of the NiO powders could be attributed to the influence of the starting materials, the temperature, or the time of calcination. It can be seen that the nickel precursor has a large influence on the structural shape of NiO crystals (Fig. 3).

The NiO obtained from the nickel acetate is more crystalline than the nitrate. Therefore, the polarity of the nickel acetate is greater than the nickel nitrate. The polarity of a molecule serves as a rough estimate of its solubility in a solvent with different polarity; in this case, the nickel acetate was more soluble than the nitrate.

The effect of starting material can be explained as follows: the nickel acetate is surrounded by a large amount of OH^- and the nucleation of Ni(OH)$_2$ would be very fast, whereas the particle growth is restricted by surrounding OH^- to result in small Ni(OH)$_2$ crystallites. The freshly formed Ni(OH)$_2$ would decompose rapidly and thus NiO nanocrystals are produced. If the starting material has a low polarity, the OH^- concentration around Ni^{2+} decreases, and the nucleation of Ni(OH)$_2$ slows down. As a result, the NiO that is produced is more regular in shape and much larger in size.

The BET surface area of the product shows that NiO particles prepared from the nickel acetate or nitrate in the presence of hydrogen peroxide had a high specific surface area (33 and 25 $m^2 g^{-1}$, respectively). This surface area was 6 times higher than the NiO obtained in the presence of KOH or NaOH, from other nickel salts, such as $Ni(NO_3)_2$ and $NiCl_2$, which was in the range of 5.2 – 5.5 $m^2 g^{-1}$, and it was 15 times higher than that from $NiSO_4$, which was in the range of 2.9 – 3.9 $m^2 g^{-1}$ [10,12].

In this way, using nickel salts (acetate or nitrate) as precursors in the presence of H_2O_2 yielded the crystalline NiO particles. NiO particles obtained in this study were larger than NiO obtained from other nickel salts, such as $Ni(NO_3)_2$, $NiCl_2$, and $NiSO_4$ in the presence of NaOH or KOH. The NiO crystal size can be increased with the calcination temperature. In this study, H_2O_2 was found to be the most appropriate reagent for the nickel oxide synthesis, because it produced the most uniformly-sized particles.

Catalytic Activity of NiO

It is known that nickel oxide is an electrocatalyst for organic compounds [17,18]. It is believed that this composite material may retain and enhance the catalytic properties of the nickel oxide through fine dispersion of the catalyst particles into the conductive PAni matrix to result in a drastic increase in surface area. Additionally, the conductive PAni matrix, being closely associated to the nickel oxide catalyst as a result of co-deposited film, is expected to facilitate electron transfer during the electrocatalytic reaction. These effects were demonstrated in the catalytic oxidation of methanol in alkaline media. The cyclic voltammetric (CV) behaviour of massive nickel electrode in 0.1 mol L^{-1} NaOH is shown in Figure 4.

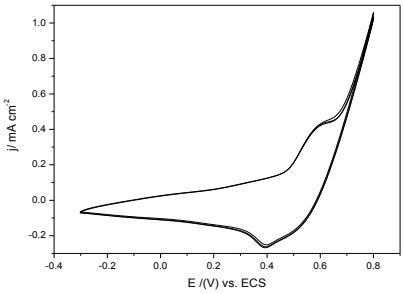

Fig. 4. CV behaviour of massive nickel electrode in 0.1 mol L^{-1} NaOH.

Polarization was started by potential scanning at a scan rate of 100 mV s−1 from −300 to 800 mV in the anodic direction and then the scan was reversed in the cathodic direction back to −300 mV. As reported by Abdel Rahim et al [18], in this work, a peak at 570mV was also observed in the positive potential and another one at 400 mV in the anodic and the cathodic directions, respectively. This couple of peaks corresponds to the oxidation of Ni(OH)2 to NiOOH (Eq. 2) [15,16,19]. Figure 5 shows data obtained during the electro-oxidation of methanol monitored by cyclic voltammetry.

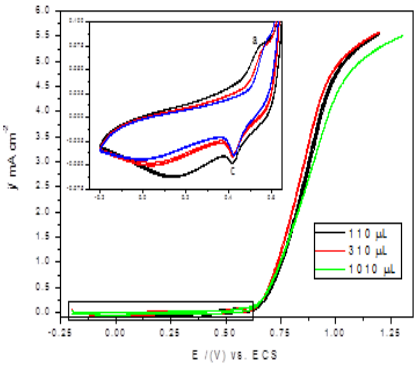

Fig. 5. CV of methanol oxidation on NiO and PANI/NiO electrodes at 100 mV s^{-1}.

An oxidation process occurs with a marked current and in the positive potential area, with the formation of a level where the process is likely to achieve a current limit by diffusion. The process is totally irreversible, once the curve shows a small hysteresis, suggesting that the alcohol oxidation occurs with the formation of CO_2 (gas) that cannot be reduced.

On the addition of the substrates, the large anodic current increases, which corresponded to the Ni(II) to Ni(III) transition, indicating that electro-catalytic oxidation of the alcohols had occurred. The catalytic anodic reactions are summarized as follows [19]:

$$NiO + 2OH^- \rightarrow Ni(OH)_2 + 2e^- \quad \text{Eq. 1}$$

$$Ni(OH)_2 + OH^- \rightarrow NiO(OH) + H_2O + e^- \quad \text{Eq. 2}$$

$$NiO(OH) + \text{organic compound} \xrightarrow{Slow} Ni(OH)_2 + \text{product}^- \quad \text{Eq. 3}$$

As it can be observed (Fig. 5), addition of methanol to the electrolyte, causes an increase in the I_{pa} and decrease in the I_{pc}. There is also an oxidizing process at a potential, more positive than the oxidation derived from Ni(II)/Ni(III), which is related to the oxidation of methanol. The presence of I_{pc} indicates that the electro-oxidation of methanol at the electrode surface occurs slowly. As reported in the literature, experiments carried out to study the electro-chemical oxidation of methanol on massive nickel electrode show that such electrode is not an efficient catalyst for this reaction. This occurs because of the difficulty to measure the oxidation current of methanol on smooth nickel, because it is difficult to obtain an adsorbed oxygen-free surface [57, 64].

This behavior was observed in this work and, before the deposition of nickel of the electrode, this system was examined. Addition of methanol to the electrolyte changes the voltammetric response of the modified electrode (PAni/Ni electrode).

Conclusion

NiO nanocrystals were successfully prepared using the hydrothermal method at low temperatures of reaction and calcination. The type of starting material has a strong influence on the formation of hydroxides. The higher the polarity of the starting material, the higher the velocity of salvation, which results in a greater velocity of $Ni(OH)_2$ formation. Although not investigated in this work, temperature and time also influence the formation of the final products. The synthesis technique has the following advantages: 1) it is a simple, one-step synthesis approach, making it easy to control the growth kinetics; 2) the synthesis needs no sophisticated equipment since it is conducted at a low growth temperature of 200 ^oC under normal atmosphere; 3) as the reaction medium is the most important aspect in any reaction, using a universal solvent (water) as a medium, means that the synthesis process is non-toxic and does not produce hazardous waste. Therefore, this technique can be expanded to provide a general, simple, and convenient strategy for the synthesis of nanostructures of other functional materials with important scientific and technological applications.

The unmodified PAni electrode shows no activity for the methanol oxidation reaction in 0.1 mol L^{-1} NaOH. However, the nickel-modified PAni electrode is a good catalyst for this reaction and high current densities can be reached. The height of the oxidation peak of methanol increases by increasing the alcohol concentration. The results indicate that the reaction of the electro-oxidation of methanol is an activation-controlled proceeding by a direct chemical reaction with NiO(OH) for thin nickel oxides and by charge transfer with the electrode for thick oxides.

References

[1] P.V. Kamat, Chem. Rev. Vol. 93 (1993), p. 267.
[2] K.J. Kjabunde, J. Stark, O. Koper, C. Mohs, G.P. Dong, S. Decker, Y. Jiang, I. Lagadic, D. Zhang: J. Phys. Chem. Vol. 100 (1996) 12142.
[3] Z.H. Liang, Y.J. Zhu, X.L. Hu: J. Phys. Chem. B Vol. 108 (2004), p. 3488.

[4] X. Wang, J.M. Song, L.S. Gao, J.Y. Jin, H.G. Zheng, Z.D. Zhang: Nanotechnology Vol. 16 (2005), p. 37.
[5] A. Nakasa, E. Suzuki, H. Usami, H. Fujimatsu: Chem. Lett. Vol. 34 (2005), p. 428.
[6] H.J. Liu, T.Y. Peng, D.E. Zhao, K. Dai, Z.H. Peng: Mater. Chem. Phys. Vol. 87 (2004), p. 81.
[7] Q. Yang, J. Sha, X.Y. Ma, D.R. Yang: Mater. Lett. Vol. 59 (2005), p. 1967.
[8] J.H. Liang, Y.D. Li: Chem. Lett. Vol. 32 (2003), p. 1126.
[9] J. Park, E. Kang, S. Son, H. Park, M. Lee, J. Kim, K. Kim, H. Noh, J.H. Park, C. Bae, J.G. Park, T. Hyeon: Adv. Mater. Vol. 17 (2005), p. 429.
[10] C. An, R. Wang, S. Wang, Y. Liu: Mat. Res. Bull. Vol. 43 (2008), p. 2563.
[11] M.V. Kulkarni, A.K. Viswanath, R. Marimuthu, T. Seth: Polymer Eng. Sci. Vol. 44 (2004), p. 1676.
[12] L. Lutterotti, P. Scardi, P. Maistrelli: J. Appl. Crystallogr. Vol. 25 (1992), p. 459.
[13] S.D. Kirik, S.V. Borisov, V.E. Fedorov: J. Structural Chem. Vol. 22 (1981), p. 249.
[14] F.J. Torres, J.M. Amigo, J. Alarcón: J. Solid State Chem. Vol. 173 (2003), p. 40.
[15] F.C. Fonseca, D.Z. Florio, V. Esposito, E. Traversa, E.N.S. Muccillo, R. Muccillo: J. Electrochem. Soc. Vol. 153 (2006), p. A354.
[16] A.V. Radha, O. Bomati-Miguel, S.V. Ushakov, A. Navrotsky, P. Tartaj: J. Am. Ceram. Soc. Vol. 92 (2009), p. 133.
[17] S. Berchmans, H. Gomathi, G.P. Rao: J. Electroanal. Chem. Vol. 394 (1995), p. 267.
[18] T.R.I. Cataldi, D. Centonze: Anal. Chim. Acta Vol. 307 (1995), p. 43.
[19] O. Enea: Electrochim. Acta Vol. 35 (1990), p. 375.